Studies of NO−Char Reaction Kinetics Obtained from Drop-Tube Furnace and Thermogravimetric Experiments

ARTICLE *in* ENERGY & FUELS · DECEMBER 2008

Impact Factor: 2.79 · DOI: 10.1021/ef800695k

7 AUTHORS, INCLUDING:

Shaozeng Sun
Harbin Institute of Technology
45 PUBLICATIONS **367** CITATIONS

SEE PROFILE

Juwei Zhang
IHI Corporation
22 PUBLICATIONS **179** CITATIONS

SEE PROFILE

Jiancheng Yang
Hebei University of Technology
2 PUBLICATIONS **18** CITATIONS

SEE PROFILE

Studies of NO−Char Reaction Kinetics Obtained from Drop-Tube Furnace and Thermogravimetric Experiments

Shaozeng Sun,[†] Juwei Zhang,*[,†] Xidong Hu,[†] Shaohua Wu,[†] Jiancheng Yang,[†] Yang Wang,[‡] and Yukun Qin[†]

Combustion Engineering Research Institute, School of Energy Science and Engineering, Harbin Institute of Technology, 92, West Dazhi Street, Harbin 150001, People's Republic of China, and State Technology Research Center of Combustion of Power Plant, Shengyang 110034, Liangning Province, People's Republic of China

Received August 22, 2008. Revised Manuscript Received October 24, 2008

Four coal chars were prepared in a flat flame flow reactor (FFR), which can simulate the temperature and gas composition of a real pulverized coal combustion environment. The pore structure of chars was measured by mercury porosimetry and nitrogen adsorption, and the Hg and Brunauer−Emmett−Teller (BET) surface areas were obtained. The kinetics of NO−char was studied in a drop-tube furnace (DTF) and thermogravimetric analyzer (TGA). In the TGA experiments, the random pore model (RPM) was applied to describe the NO−char reactions and obtain the intrinsic kinetics. By presenting the data of DTF and TGA experiments on the same Arrhenius plot, it can be concluded that TGA is an available tool to study the kinetics of a high-temperature NO−char reaction. With respect to the DTF experiments, in comparison to the BET surface area, the Hg surface area is a better basis for normalizing the reactivity of different coal chars because of less scatter in the measured values, better agreement with TGA experimental data, and more stable values during the process of reaction. Moreover, by comparing the Hg surface area of chars before and after reactions, it is believed that the Hg surface area basis is more appropriate for high-rank coal chars. The determined kinetic rate constants are in good agreement with other data in the literature, and a new rate constant expression is proposed.

1. Introduction

The reaction of nitrogen monoxide with char is of special interest because of its importance in producing or reducing NO emission from combustion systems, such as fluidized beds or pulverized coal combustion boilers.[1−3] Despite considerable previous work in the literature about the reduction of nitrogen monoxide by char, the mechanism of the reaction is still not clearly understood and there are large variations in reaction data.[4] These variations can be attributed to the existence of many factors, such as the rank of the parent coal, the inherent catalytic mineral matter, mass-transfer limitations at high temperatures, and the effects of other gases on char reactivity.

Several types of experimental apparatuses have been used to explore the NO−char reaction rate and to determine the kinetic parameters. Among these apparatuses, fixed beds were most widely adopted.[5−12] However, most published studies that were conducted in a fixed bed focused on temperatures typically found in fluidized beds (873−1273 K) rather than temperatures in an industrial pulverized coal-fired furnace (above 1473 K). To study a high-temperature NO−char reaction, it is preferable to use a drop tube furnace (DTF). Moreover, the heating rates in DTF (above 10^4 K/s) are close to those found in a full-scale pulverized coal-fired furnace. Thus far, only a few studies have been performed at high temperature above 1273 K, and DTF was used in all of these studies. Song et al.[13] studied the NO−char reaction in a flow reactor in the temperature range of 1250−1750 K and concluded that the order of the reaction was unity with respect to NO. Levy et al.[14] measured the reaction rate in the temperature range of 1250−1750 K and concluded that the NO−char reaction was slightly sensitive to variations in the gas composition and the presence of carbon monoxide enhanced the reaction, whereas water had an inhibitory effect. Schonenbeck et al.[15] studied the heterogeneous reaction between NO and a coal char in the temperature range of 1273−1573 K in a DTF. The results supported the assumption of a first-order reaction with respect to the NO concentration and surface area

* To whom correspondence should be addressed: Combustion Engineering Research Institute, School of Energy Science and Engineering, Harbin Institute of Technology, 92, West Dazhi Street, Harbin 150001, People's Republic of China. Telephone: +86-451-8641-2908, ext. 856. Fax: +86-451-8641-2528. E-mail: zhangjw@hit.edu.cn.

[†] Harbin Institute of Technology.

[‡] State Technology Research Center of Combustion of Power Plant.

(1) Smoot, L. D.; Hill, S. D.; Xu, H. *Prog. Energy Combust. Sci.* **1998**, *24* (5), 385–408.

(2) Zhong, B. J.; Zhang, H. S.; Fu, W. B. *Combust. Flame* **2003**, *132* (3), 364–373.

(3) Xie, G. L.; Fan, W. D.; Song, Z. L.; Lu, J.; Yu, J.; Zhang, M. C. *Energy Fuels* **2007**, *21* (6), 3134–3143.

(4) Aarna, I.; Suuberg, E. M. *Fuel* **1997**, *76* (6), 475–491.

(5) Chambrion, P.; Suzuki, T.; Zhang, G. Z.; Kyotani, T.; Tomita, A. *Energy Fuels* **1997**, *11* (3), 681–685.

(6) Wu, S. L.; Iisa, K. *Energy Fuels* **1998**, *12* (3), 457–463.

(7) Aarna, I.; Suuberg, E. M. *Energy Fuels* **1999**, *13* (6), 1145–1153.

(8) Liu, H.; Kojima, T.; Feng, B.; Liu, D. C.; Lu, J. D. *Energy Fuels* **2001**, *15* (3), 696–701.

(9) Sorensen, C. O.; Johnsson, J. E.; Jensen, A. *Energy Fuels* **2001**, *15* (6), 1359–1368.

(10) Garijo, E. G.; Jensen, A. D.; Glarborg, P. *Energy Fuels* **2003**, *17* (6), 1429–1436.

(11) Lopez, D.; Calo, J. *Energy Fuels* **2007**, *21* (4), 1872–1878.

(12) Dong, L.; Gao, S. Q.; Song, W. L.; Xu, G. W. *Fuel Process. Technol.* **2007**, *88* (7), 707–715.

(13) Song, Y. H.; Beer, J. M.; Sarofim, A. F. *Combust. Sci. Technol.* **1981**, *25*, 237–340.

(14) Levy, J. M.; Chan, L. K.; Sarofim, A. F.; Beer, J. M. Eighteenth International Symposium on Combustion, The Combustion Institute, Pittsburgh, PA, 1980; pp 111−120.

(15) Schonenbeck, C.; Gadiou, R.; Schwartz, D. *Fuel* **2004**, *83* (4), 443–450.

10.1021/ef800695k CCC: $40.75
Published on Web 12/05/2008

of char, and the activation energy was determined by a combination of the experiment and computational fluid dynamics (CFD) simulation. Zhong and Tang[16] studied the effect of single-metal oxides contained in coal ashes on NO reduction in the high-temperature range of 1223−1523 K in a DTF. The results showed that the catalysts had a great positive effect on NO reduction and that catalytic activity of KOH was slightly better than that of NaOH.

In addition, some simple and rapid tests, such as the thermogravimetric analyzer (TGA), can also be used to study the NO−char reaction. Li et al.[17] studied the kinetics of the NO−char reaction in a TGA and introduced a new model by taking into account the contribution from different carbon−oxygen surface complexes during the reaction. Wang et al.[18] investigated the reactions of carbonaceous materials (graphon and coal char) with NO, O_2, and NO + O_2 by a TGA. In addition, a method of direct nonlinear regression of the kinetic equation was applied to obtain kinetic parameters from the TG curve of carbon gasification in various atmospheres.

In this study, the isothermal kinetic experiments were performed in both DTF and TGA. The results obtained by DTF were compared to those obtained by TGA. The purpose of this study was to explore the kinetics of the NO−char reaction in a wide temperature range of 973−1573 K and investigate whether thermogravimetric analysis tests could be available to analyze the kinetics of the NO−char reaction.

2. Experimental Section

Char Preparation. Four Chinese coals, a lignite (YB coal), two bituminous coals (SH coal and SJ coal), and an anthracite (YQ coal), were used. The raw coals were sieved to obtain the 53−75 μm size fraction. The chars were prepared from these coals in a flat flame flow reactor (FFR). The FFR uses the hot products of the $CH_4/CO/O_2/N_2$ flame to heat the char particles, to approximate the temperature and gas composition of an industrial pulverized coal combustion environment as closely as possible.[19] Coal particles were pyrolyzed in a postflame zone of the flat flame operated under fuel-rich conditions (equivalence ratio $\phi = 1.4$) with almost no oxygen existing in the postflame region, so that this experiment may be more representative of the fuel-rich region in a coal flame than experiments conducted in inert gases, such as nitrogen or argon.[19,20]

A schematic of the FFR system is shown in Figure 1. The key part of the system is a McKenna flat flame burner, which is modified from a standard McKenna burner. An inner burner was added to the standard burner to introduce the particles. The inner burner was operated with the same equivalence ratio as the outer burner. The maximum particle heating rate in the FFR was 10^5 K/s. The flame temperature and postflame gas composition were measured. The flow rate settings of burners and the measured results are displayed in Tables 1 and 2. As shown in Table 2, the high temperature and high CO concentration of the flame indicate a high-temperature reducing atmosphere.

Coal particles were fed to the inner burner with a particle feeder. The feeding rate was 4−6 g/h, depending upon the bulk density of coals. This low feeding rate minimizes the interaction between particles to ensure single-particle reaction behavior. The inner burner gases (without O_2) were used to entrain the coal particles. The gas flow rates were regulated by mass flow controllers. The particle collection system included an oil-cooled, nitrogen-quenched probe followed by some gas−solid separating devices. The residence time could be changed by raising or lowering the probe. The particle residence time in this experiment was around 60 ms, which ensured that the devolatilization process was completed in the postflame zone in FFR.[21]

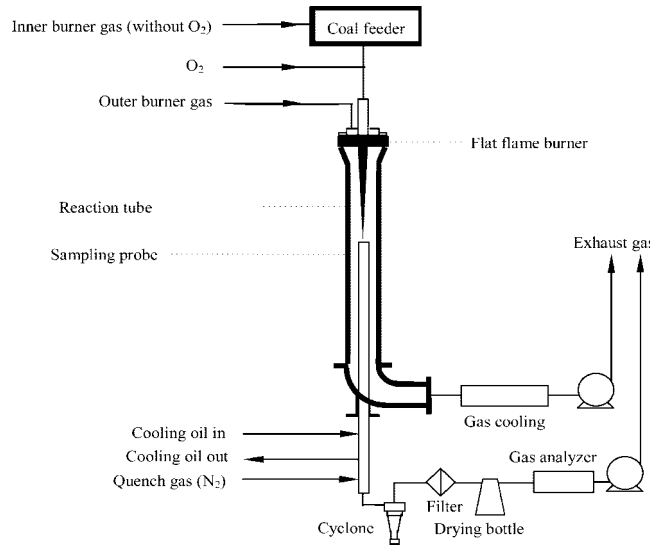

Figure 1. Schematic of FFR facility.

Table 1. Flow Rate Settings of Burners in FFR

inner burner flow rates (slpm)[a]				outer burner flow rates (slpm)			
CH_4	O_2	CO	N_2	CH_4	O_2	CO	N_2
0.06	0.16	0.19	0.74	2.0	5.0	6.0	23.0

[a] "slpm" stands for standard liters per minute (i.e., at 1 atm and 273 K).

Table 2. Measured Results of Postflame Gas in FFR

flame temperature (K)	gas composition after combustion (vol %)			
T	N_2	CO_2	H_2O	CO
1952	65.69	13.12	10.51	11.78

DTF Experiments. Experiments were performed in a high-temperature, laminar DTF. The schematic of DTF was shown in Figure 2. The alumina tube (inner diameter of 50 mm and length of 1.4 m) was adopted as the reaction tube. The furnace was heated electrically to the required temperature before every experiment. The furnace temperatures in experiments were set to 1273, 1373, 1473, and 1573 K, respectively. Char particles were entrained by N_2 (0.5 L/min, 1 atm, and 273 K) into the furnace at a feeding rate of about 5−20 g/h depending upon the bulk density of chars. A gas flow (5 L/min, 1 atm, and 273 K) consisting of NO and N_2 was preheated to 873 K before being introduced into the hot zone of the furnace. The initial NO concentration was set to 1040 ppmv. Reaction products were sampled by an oil-cooled, nitrogen-quenched probe, and the composition of exhaust gases were measured by an online Fourier transform infrared (FTIR) gas analyzer (GASMET-DX4000, Finland). The sampling point was fixed to the position that is 600 mm away from injection port, and the residence time is 2.23−2.75 s depending upon temperatures.

According to previous studies, the reaction of NO with coal char is found to be first-order with respect to NO.[4,13,15] The rate of NO consumption $-r_{NO}$ can be defined as

$$-r_{NO} = \eta k Y A m p_{NO} \quad (1)$$

Equation 1 can be integrated to give

$$\eta k = \frac{-\ln(1-x)}{YAmtRT} \quad (2)$$

(16) Zhong, B. J.; Tang, H. *Combust. Flame* **2007**, *149* (1−2), 234–243.

(17) Li, Y. H.; Radovic, L. R.; Lu, G. Q.; Rudolph, V. *Chem. Eng. Sci.* **1999**, *54* (19), 4125–4136.

(18) Wang, S. B.; Slovak, V.; Haynes, B. S. *Fuel Process. Technol.* **2005**, *86* (6), 651–660.

(19) Zeng, D.; Clark, M.; Gunderson, T.; Hecker, W. C.; Fletcher, T. H. *Proc. Combust. Inst.* **2005**, *30*, 2213–2221.

(20) Fletcher, T. H.; Ma, J. L.; Rigby, J. R.; Brown, A. L.; Webb, B. W. *Prog. Energy Combust. Sci.* **1997**, *23* (3), 293–301.

(21) Ma, J. L. Ph.D. Thesis, Brigham Young University, Provo, UT, 1996.

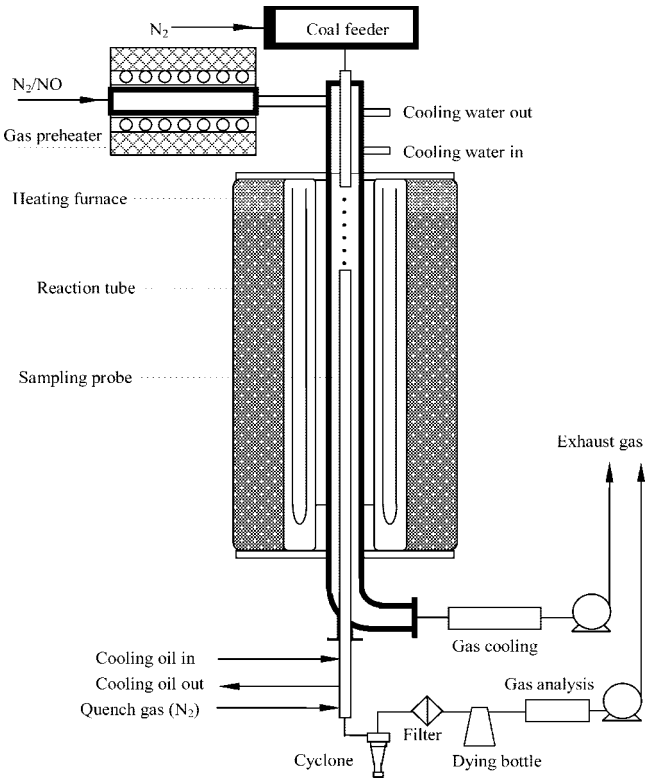

Figure 2. Schematic of DTF facility.

As in eq 2, k is a pseudo-constant, whose value depends upon T, and the influence of T on RT is negligible compared to that on k. Therefore, the values of k can be presented in Arrhenius plots as straight lines. Then, k can be expressed in Arrhenius form as follows:

$$k = k_0 \exp\left(-\frac{E}{RT}\right) \tag{3}$$

If $-r_{NO}$ is expressed in terms of the NO molar concentration C_{NO}

$$-r_{NO} = \eta k' YAmC_{NO} \tag{4}$$

and the intrinsic rate coefficient k' is in m/s

$$\eta k' = \frac{-\ln(1-x)}{YAmt} \tag{5}$$

Then

$$k' = kRT \tag{6}$$

Although the diameter of char particles is very small, the pore diffusion limitation must be taken into account because of the high reaction temperatures. The effective diffusion coefficient is expressed as follows:

$$D_{eff} = \frac{\theta}{\tau}\left(\frac{1}{D_m} + \frac{1}{D_k}\right)^{-1} \tag{7}$$

Knudsen diffusion coefficient D_k can be defined as follows:

$$D_{knu} = \frac{2r_e}{3}\sqrt{\frac{8RT}{\pi M_{NO}}} \tag{8}$$

where r_e is an empirical mean pore radius according to the pore model proposed by Satterfield,[22] and it can be defined as follows:

$$r_e = \frac{2\theta}{A\rho_P} \tag{9}$$

Before calculating the effectiveness factor η, Thiele diffusion modulus φ_s should be determined

$$\varphi_s = d_P\sqrt{\frac{k'\rho_p YA}{D_{eff}}} \tag{10}$$

Then, the effectiveness factor η can be determined

$$\eta = \frac{3}{\varphi_s}\left(\frac{1}{\tanh\varphi_s} - \frac{1}{\varphi_s}\right) \tag{11}$$

The value of k or k' can be obtained from eqs 2, 10, and 11 by trial and error. According to the theories mentioned above, the kinetic parameters of the NO−char can be obtained.

TGA Experiments. YB char (from YB coal) and SH char were used in this experiment. Reactivity measurements of the chars were carried out in a TGA (Mettler-Toledo TGA/SDTA851^e, Switzerland) by isothermal analysis. Argon (99.999% purity) was used as the purge and balance gas. About 1 mg of char was placed in an alumina pan. The gas flow rate was maintained at 250 mL/min, and the NO concentration was 1% (v/v). The sample was degassed at 323 K for 80 min before the experiment. After degassing, the temperature was raised to reaction temperatures, which ranged from 973 to 1573 K. The mixture of a specific NO concentration was introduced into the furnace after the mass of the sample was stabilized. The weight of the sample was recorded continuously as a function of time. Preliminary runs were carried out to determine the proper values of sample mass and gas flow rate to eliminate bulk diffusion limitations.

According to the model that is proposed by Li et al.[17] and on the basis of the random pore model (RPM),[23] the specific reaction rate R_C under constant NO concentration can be expressed as follows:

$$R_C = \frac{1}{1-X}\frac{dX}{dt} = k_C\sqrt{1-\psi\ln(1-X)} \tag{12}$$

The rate constant k_C and pore structure parameter ψ can be obtained by fitting the experimental data at various temperatures to eq 12.

Char Characterization Measurements. The complete pore structure for all char samples was obtained by combining porosimetry with gas adsorption. Macropore/mesopore surface area and pore volume were measured by mercury porosimetry (Autopore II 9220, Micromeritics, Norcross, GA). Nitrogen adsorption at 77 K was performed in an automated adsorption analyzer (ASAP 2020, Micromeritics, Norcross, GA), and the specific surface area was calculated by the Brunauer−Emmett−Teller (BET) equation. The true density was measured by a helium pycnometer (AccuPyc 1330, Micromeritics, Norcross, GA). The mass mean diameter ($D_{4,3}$) of char particles was estimated by a laser size analyzer (Master Min, Malvern, U.K.). The results are given in Table 3. It should be noted that the specific surface areas of YB and SH chars are obviously higher than the other two chars, which can be attributed to higher volatiles and lower rank of their parent coals.[24]

3. Results and Discussion

Reaction of Chars with NO. The NO−char reaction is described by the following overall reactions:

$$2NO + C \rightarrow N_2 + CO_2 \tag{13}$$

$$NO + C \rightarrow 1/2N_2 + CO \tag{14}$$

The CO/CO_2 ratio has been observed to begin at values less than 1 and to increase monotonically with temperature,[4,6,11] just

(22) Satterfield, C. N. *Mass Transfer in Heterogeneous Catalysis*; MIT Press: Cambridge, MA, 1970.

(23) Bhatia, S. K.; Perlmutter, D. D. *AIChE J.* **1980**, *26* (3), 379–386.

(24) Yu, J. L.; Lucas, J. A.; Wall, F. W. *Prog. Energy Combust. Sci.* **2007**, *33* (2), 135–170.

Table 3. Properties of Chars Prepared from FFR

properties	YB char	SH char	SJ char	YQ char
Proximate Analysis (db)				
volatiles (%)	14.2	11.1	9.3	5.8
ash (%)	31.3	10.6	56.4	11.6
fixed carbon (%)	54.5	78.3	34.3	82.5
Ultimate Analysis (daf)				
carbon (%)	92.1	92.6	93.9	94.1
hydrogen (%)	3.6	2.3	2.5	2.2
nitrogen (%)	1	0.9	1.5	1.3
sulfur (%)	1.5	1.4	1.6	1.8
Specific Surface Area ($m^2\ g^{-1}$)				
BET	217.7	244.4	70.0	26.2
Hg[a]	18.2	11.1	6.9	2.0
mass mean diameter (μm)	52.9	53.3	50.8	46.5
true density (kg m^{-3})	2215	1586	2065	1833
porosity	0.845	0.784	0.746	0.557

[a] The specific surface area of pores larger than 20 nm.

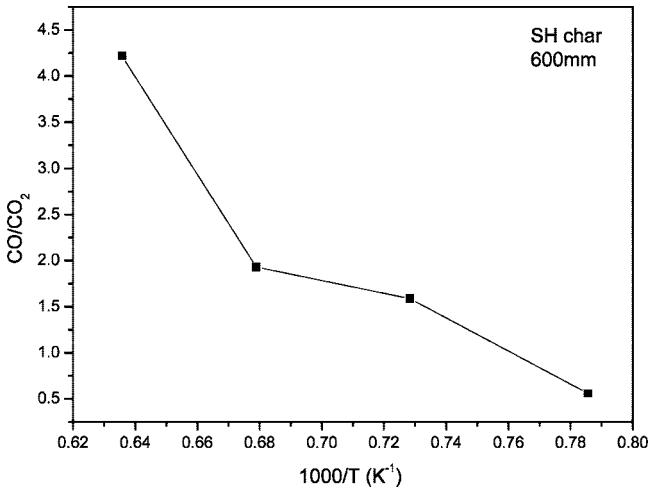

Figure 3. Influence of the temperature on the CO/CO_2 ratio (from DTF experiments).

as in the case of carbon gasification in oxygen. Figure 3 shows that the influence of the temperature on the CO/CO_2 ratio is obvious. The CO/CO_2 ratio at 1273 and 1373 K was 0.56 and 1.59; therefore, reaction 13 was the major reaction below 1273 K, and reaction 14 was the major reaction above 1373 K.

Figure 4 shows the Arrhenius plots of YB char and SH char at various carbon conversion levels. A good linear relationship can be obtained for all cases. It is observed that there are two temperature regimes of activation energy for all cases. The transition temperature for both chars is 1173 K. The activation energies evaluated below 1173 K are obviously higher than that evaluated above 1173 K. In addition, the variations of activation energies indicate that the reactions were under chemical kinetics control in the low-temperature regime (below 1173 K) and under diffusion control in the high-temperature regime (above 1173 K). In this study, to obtain the intrinsic kinetic parameters, only the data in the low-temperature regime were used.

The rate constant k_C and pore structure parameter ψ were obtained by fitting the experimental data at various temperatures to eq 12. The results are shown in Table 4. According to the Arrhenius equation, the activation energies and pre-exponential factors were obtained from k_C and the Arrhenius plots in terms of k_C for both chars are shown in Figure 5. The good linear relationship obtained for chars confirmed that the reactions of both chars in the low-temperature regime were under chemical kinetics control.

In Figure 6, experimental results of reaction rates versus carbon conversion are compared to the predictions by the RPM.

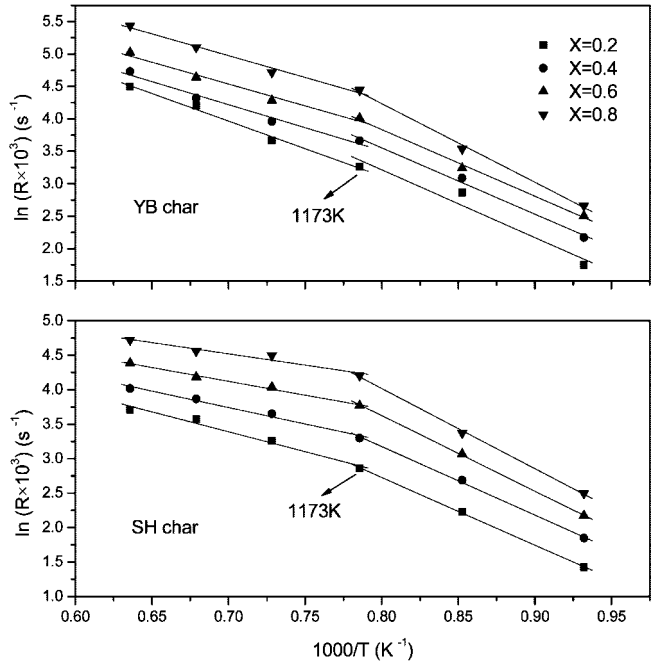

Figure 4. Arrhenius plots of NO−char reaction at various carbon conversion (from TGA experiments).

Table 4. Kinetic Parameters from the RPM (from TGA Experiments)

	YB char		SH char	
reaction temperature (K)	$k_C \times 10^3$ ($g\ g^{-1}\ s^{-1}$)	ψ	$k_C \times 10^3$ ($g\ g^{-1}\ s^{-1}$)	ψ
973	1	10	0.35	36.01
1073	3.32	9.09	1.48	35.45
1173	11.83	4.3	3.61	31.38
activation energy (kJ/mol)	116.8		121.5	
pre-exponential factor ($g\ g^{-1}\ s^{-1}$)	1.78×10^3		1.03×10^3	

For both chars, the shape of the predicted curves is in good agreement with that of the experimental data at different temperatures. However, RPM underestimates the experimental results at high carbon conversions, and the maximum reaction rate is shifted toward higher conversions. This is attributed to the catalytic effects of inherent minerals in chars. According to mathematical analysis of RPM by Bhatia and Perlmutter,[23] the

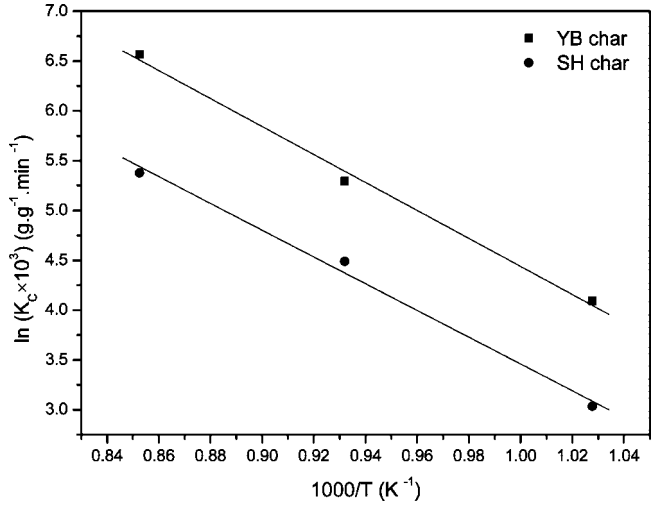

Figure 5. Arrhenius plots of the NO−char reaction from the RPM (from TGA experiments).

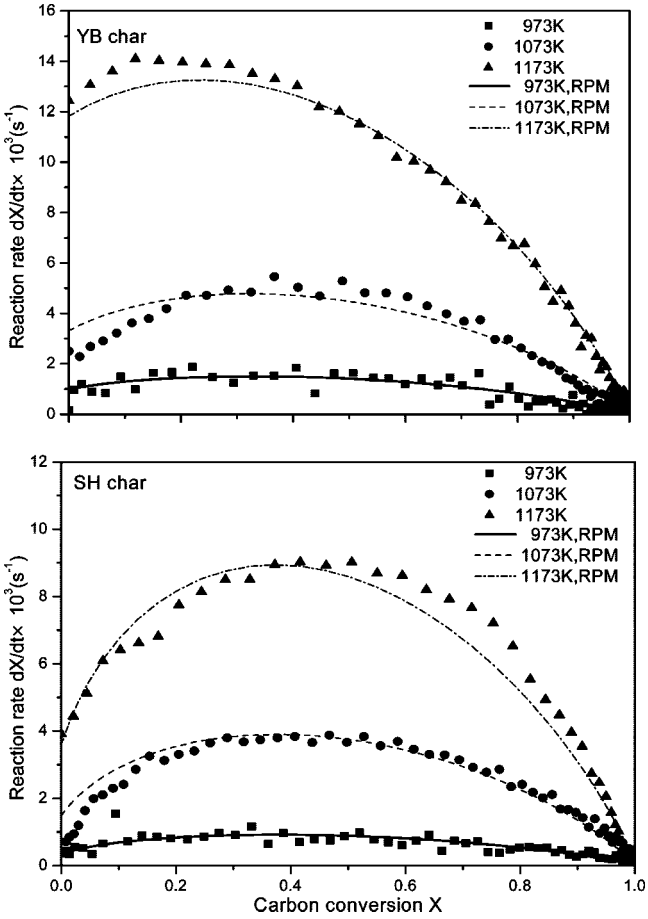

Figure 6. Experimental and fitted reaction rates as a function of carbon conversion (from TGA experiments).

Table 5. Effectiveness Factors for the NO−Char Reactions in DTF

	1273 K		1373 K		1473 K		1573 K	
	η_{BET}	$\eta_{Hg}{}^a$	η_{BET}	$\eta_{Hg}{}^a$	η_{BET}	$\eta_{Hg}{}^a$	η_{BET}	$\eta_{Hg}{}^a$
YB char	0.374	0.829	0.283	0.759	0.174	0.615	0.143	0.548
SH char	0.621	0.947	0.367	0.872	0.244	0.802	0.141	0.659
SJ char	0.778	0.945	0.717	0.927	0.556	0.874	0.489	0.842
YQ char	0.918	0.980	0.865	0.966	0.738	0.926	0.458	0.801

[a] Calculated with the specific surface area of pores larger than 20 nm.

position of the maximum rate should be restricted to the range of $0 \le X \le 0.393$. However, previous studies[25,26] have revealed that the peak rate can be shifted toward higher conversions because of the accumulation of metal catalyst on the char surface.

For the DTF experiments, effectiveness factors for NO−char reactions were calculated with both BET (i.e., area measured by nitrogen adsorption) surface area and Hg (i.e., area measured by mercury porosimetry) surface area, and results are given in Table 5. The values in Table 5 indicate that the mass-transfer limitations have a great impact on the reactivity of chars toward NO, especially for the low-rank coal chars (YB and SH chars). Because of the higher value of the BET surface area, the effectiveness factors based on BET surface area (η_{BET}) are evidently higher than those based on Hg surface area (η_{Hg}). For the YB and SH chars, the reactions are mainly under diffusion control if η_{BET} is used but mainly under chemical kinetics control if η_{Hg} is used. Therefore, it is very important to decide which area basis is adopted to estimate the intrinsic reactivity of chars.

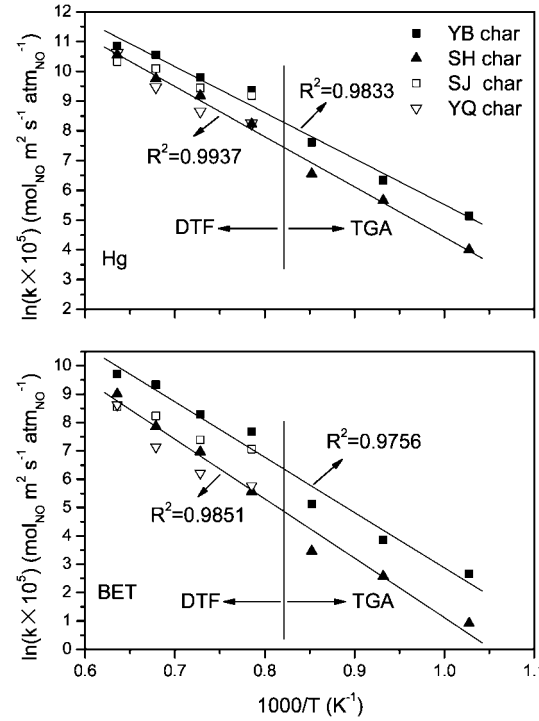

Figure 7. Comparison of Arrhenius plots using BET and Hg surface area basis.

Kinetic Analysis of DTF and TGA Experimental Data. Figure 7 shows the comparison of Arrhenius plots from different area basis for all chars. For the YB and SH chars, the results from TGA were also presented. The rate constant k_C from TGA is expressed as the mass of carbon consumed per mass of carbon remained per unit time ($g_C\ g_C^{-1}\ s^{-1}$). For the sake of comparing this rate constant to DTF experimental data, the rate constant should be transformed into units of moles of NO consumed per surface area of carbon per unit of time per unit NO pressure ($g_{NO}\ m^2\ s^{-1}\ atm_{NO}^{-1}$). Then, the new rate constant kC' is expressed as follows:

$$kC' = nk_C/(YAM_C p_{NO}) \quad (15)$$

where n is the NO/C ratio in eq 13 or 14 and set to 2 assuming that eq 13 is the overall reaction in low-temperature TGA experiments and p_{NO} is 0.00987 atm corresponding to a NO concentration of 1% (v/v) in this study.

As can be seen in Figure 7, data calculated on BET surface area basis display a wider spread of values than those calculated on Hg surface area basis, which is also found by Commandre et al.[27,28] As shown in Table 6, the values of the k_{YB}/k_{SH} ratio using Hg surface area basis at various temperatures are much closer to unity, which suggests that the Hg surface area is a better basis for normalizing the reactivity of different coal chars. In Figure 7, for the YB and SH chars, a good linear relationship can be obtained for both area basis by combining the DTF and TGA experimental data. It indicates that to some extent the high-temperature reactivity of coal chars can be extrapolated from low-temperature TGA experimental data and TGA can be used

(25) Hamilton, R.; Sams, T.; Shadman, D. A. *Fuel* **1984**, *63* (8), 1043–1047.

(26) Strius, R. P. W. J.; Scala, C. V.; Stucki, S.; Prins, R. *Chem. Eng. Sci.* **2002**, *57* (17), 3581–3592.

(27) Commandre, J. M.; Stanmore, B. R.; Salvador, S. *Combust. Flame* **2002**, *128* (3), 211–216.

(28) Salvador, S.; Commandre, J. M.; Stanmore, B. R.; Gadiou, R. *Energy Fuels* **2004**, *18* (2), 296–301.

Table 6. Comparison of the k_{YB}/k_{SH}[a] Ratio Using BET and Hg Surface Area Basis[b]

temperature (K)	k_{YB}/k_{SH} (BET)	k_{YB}/k_{SH} (Hg)
973	5.70	3.11
1073	3.61	1.97
1173	5.28	2.88
1273	8.33	3.12
1373	3.82	1.85
1473	4.35	2.21
1573	2.01	1.34

[a] The ratio of the intrinsic rate constants for YB and SH chars. [b] The data of 973, 1073, and 1173 K are from TGA experiments.

Table 7. Surface Area Variations of Chars during NO−Char Reactions (1473 K)

	YB char	SH char	SJ char	YQ char
rank of parent coal	lignite	high-volatile bituminous	low-volatile bituminous	anthracite
Hg1[a]	18.2	11.1	6.9	2.3
Hg2[b]	5.7	4.7	5.6	2.0
Hg2/Hg1	0.31	0.42	0.81	0.87
BET1[c]	217.7	244.4	70.0	26.2
BET2[d]	186.5	89.6	11.5	1.45
BET2/BET1	0.85	0.36	0.16	0.06

[a] Hg surface area of chars before reaction. [b] Hg surface area of chars collected at the gas-sampling position after reaction. [c] BET surface area of chars before reaction. [d] BET surface area of chars collected at the gas-sampling position after reaction.

to analyze the kinetics of the NO−char reaction. In fact, the reaction temperatures used in this study are all above the transition temperature, which is referenced in many studies,[4,17] and the reactions in DTF and TGA have the same reaction mechanism. Additionally, for both chars, the correlation factors (R^2) for the linear least-squares estimation calculated on Hg surface area basis are higher than those calculated on BET surface area basis, which also indicates that the Hg surface area is a better basis.

The fact that the Hg surface area is a better basis was also found in char combustion.[29,30] He et al.[30] found that the Hg surface area is approximately unchanged during char combustion. However, as shown in Table 7, Hg surface area decreases after high-temperature NO−char reactions in inert atmosphere (NO can be ignored because of its low concentration and low carbon conversion). The exposure of coal char to high temperature causes a thermal annealing of particles and increases crystallographic order of carbon, characterized by the char surface area loss or char reactivity loss (deactivation). Char deactivation involves a series of complex processes, such as carbonaceous matrix transformation, the collapse of pore wall, the fusion of inorganic matters, etc. It can be seen that the Hg2/Hg1 ratio increases monotonously when the parent coal rank increases. Therefore, the extent of char deactivation is closely associated with parent coal rank. High-rank coal has more aromatic ring structure, and low-rank coal has more aliphatic chains, which are lost rapidly in a high-temperature atmosphere. In this study, chars from the high-rank coals (SJ and YQ chars) have more ordered carbon network and less side chains; therefore, the Hg surface area of both chars decreases more slowly than

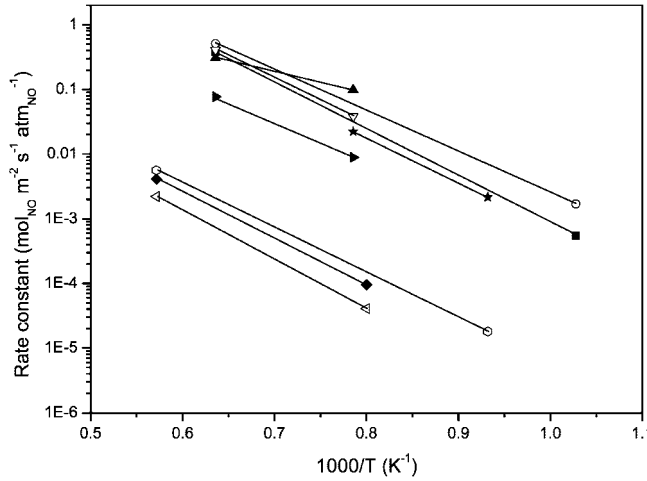

Figure 8. Summary of first-order rate constants for the NO−char reaction

the other two chars from low-rank coals. This implies that the Hg surface area basis is more appropriate for high-rank coal chars.

From Table 7, it can be seen that the BET2/BET1 ratios for almost all chars (except YB char) are higher than the corresponding Hg2/Hg1 ratios, especially for the low-rank coal chars. This is due to a different deactivation mechanism for BET surface area. It is well-known that the BET surface area is mainly associated to micro- and mesopores, whose area is easily affected by the sintering and blockage by mineral matters. This indicates that the values of Hg surface area are more stable than those of BET surface area and further supports the fact that Hg surface area is a more appropriate area basis. In addition, it is very interesting to note that the BET2/BET1 ratios decrease with the increase of parent coal rank, and this is a reverse variation trend compared to that of Hg2/Hg1 ratios. However, the cause of this behavior is not clearly understood, and it will be studied in the forthcoming work.

Figure 8 and Table 8 summarize some first-order rate constants for the NO−char reaction. All data were obtained in DTF, except the data of Aarna and Suuberg,[4] which were obtained by averaging a great deal of reported kinetic parameters. There are more than 2 orders of magnitude spread in all rate constants. However, the values of this study are in good agreement with another one calculated on Hg surface area (see Table 8). Thus, the scatter of data may also be attributed to the differences between BET and Hg surface area basis. However, there are some factors not explicitly represented in Figure 8. For example, the presence of some catalytic metal can increase the reactivity of char and decrease the activation energies of the NO−char reaction. The activation energies in this study were obtained from high-temperature DTF experiments (for YB and SJ chars, the activation energies were 129 and 140 kJ/mol, respectively, combining the DTF and TGA experimental data). As shown in Table 8, the activation energies of YB and SJ chars were apparently lower than others, which is attributed to their higher ash content (i.e., catalytic metal; see Table 3) than other chars. In fact, it might be more valid to express the char reactivity on a catalyst-surface-area basis. However, such a conversion is impossible, because the catalytic surface area is rarely determined.

As mentioned above, the Hg surface area basis is more appropriate for high-rank coal chars. Therefore, YQ char,

(29) He, R.; Xu, X. C.; Chen, C. H.; Fan, H. L.; Zhang, B. *Fuel* **1998**, *77* (12), 1291–1295.
(30) He, R.; Suda, T.; Fujimori, T.; Sato, J. *Int. J. Heat Mass Tansfer* **2003**, *46* (19), 3619–3627.

Table 8. Key to Figure 8

symbol	char type	reactor	temperature range (K)	activation energy (kJ/mol)	surface area basis	reference
■	high-volatile bituminous coal char (SH char)	DTF and TGA	973−1573	125	Hg	this study
○	lignite coal char (YB char)	DTF and TGA	973−1573	86	Hg	this study
▲	low-volatile bituminous coal char (SJ char)	DTF	1273−1573	68	Hg	this study
▽	anthracite coal char (YQ char)	DTF	1273−1573	129	Hg	this study
◆	Montana lignite char	DTF	1250−1750	147	BET (external)	10
tilted △	Montana lignite char	DTF	1250−1750	137	BET (external)	11
tilted ▼	sub-bituminous coal char	DTF	1273−1573	120	BET	12
◇	several kinds of carbons	DTF and fixed bed	1073−1750	133		1
★	low-volatile bituminous coal char	DTF	1073−1273	131	Hg	23

which has a lower ash content than another high-rank coal char (SJ char), was used to determine the intrinsic rate constant, and the recommended intrinsic rate constant is represented as

$$k = 6.14 \times 10^3 \exp(-15539/T) \quad \mathrm{mol_{NO}\ m^{-2}\ s^{-1}\ atm_{NO}^{-1}} \tag{16}$$

To our surprise, this expression is in perfect agreement with that proposed by Commandre et al.[27] (the activation energy in this study is a little lower), although the temperatures in their experiments are lower than the temperatures in this study.

4. Conclusions

The char samples were obtained from four Chinese coals in a FFR that can simulate a real pulverized coal combustion environment. The kinetics of the NO−char reaction was studied in both DTF and TGA, and some conclusions can be drawn as follows: (1) YB and SH chars were used in the TGA experiment. The random pore model can be used to describe the reaction of all chars satisfactorily but underestimates the reaction rates at high carbon conversions for YB and SH chars, which is attributed to the accumulation of metal catalyst on the char surface. (2) For DTF experiments, the calculated effectiveness factors indicate that mass-transfer limitations have a great effect on the reactivity of chars with NO. Different surface area bases result in great differences in values of effectiveness factors. For example, for the SH char reactions, the effectiveness factors using BET surface area have values of 0.141−0.621, while the effectiveness factors using Hg surface area have values of 0.659−0.947. (3) A comparison of TGA and DTF experimental data for kinetic analysis suggests that thermogravimetric analysis is a rapid and simple method for studying the reactivity of coal char toward NO at high temperatures. (4) Presenting results on Hg surface-area-normalized basis leads to better reduction of data scatter (there is less than 1 order of magnitude spread of rate constants) compared to those on BET surface-area-normalized basis. In addition, the values of Hg surface area are more stable during the process of reaction than those of BET surface area. These all indicate that Hg surface area is a better basis for normalizing the reactivity of different coal chars. (5) The deactivation of chars during the high-temperature NO reaction was observed. The extent of char deactivation is closely associated with parent coal rank. As the coal rank increases, the Hg2/Hg1 ratios increase monotonously from 0.31 to 0.87, which implies that the Hg surface area basis is more appropriate for high-rank coal chars. (6) When rate constants in this study were compared to others from the literature, the obtained intrinsic rate constant is expressed as

$$k = 6.14 \times 10^3 \exp(-15539/T) \quad \mathrm{mol_{NO}\ m^{-2}\ s^{-1}\ atm_{NO}^{-1}}$$

Acknowledgment. This work is sponsored by the Ministry of Science and Technology of China through the National Basic Research Program of China (contract No: 2006CB200303), the National High Technology Research and Development of China (contract No: 2007AA05Z336), Natural Science Foundation of China (contract No: 50576020), and the program of excellent Team in Harbin Institute of Technology.

Nomenclature

$-r_{NO}$ = rate of NO consumption ($mol_{NO}\ m^{-3}\ s^{-1}$)
η = effectiveness factor (dimensionless)
k = intrinsic rate constant (mol $m^{-2}\ s^{-1}\ Pa^{-1}$ or mol $m^{-2}\ s^{-1}\ atm^{-1}$)
Y = mass fraction of carbon in the char particle (dimensionless)
A = specific area of char ($m^2\ g^{-1}$)
m = char mass per unit volume of furnace ($g\ m^{-3}$)
p_{NO} = the bulk partial pressure of NO (Pa or atm)
x = NO conversion (dimensionless)
t = residence time of char particles (s)
R = gas constant ($J\ mol^{-1}\ K^{-1}$)
T = temperature (K)
k_0 = pre-exponential factor (mol $m^{-2}\ s^{-1}\ Pa^{-1}$ or mol $m^{-2}\ s^{-1}\ atm^{-1}$)
E = activation energy (kJ/mol)
C_{NO} = NO molar concentration ($mol\ m^{-3}$)
k' = intrinsic rate coefficient (m/s)
θ = porosity (dimensionless)
τ = tortuosity (dimensionless)
D_m = molecular diffusion coefficient ($m^2\ s^{-1}$)
D_k = Knudsen diffusion coefficient ($m^2\ s^{-1}$)
M_{NO} = molecular mass of NO ($kg\ mol^{-1}$)
r_e = empirical mean pore radius (m)
ρ_P = apparent density of char ($m^3\ g^{-1}$)
ϕ_s = Thiele diffusion modulus (dimensionless)
d_P = averaged diameter of char particles (m)
R_C = specific reaction rate ($g\ g^{-1}\ s^{-1}$)
X = carbon conversion (dimensionless)
k_C = rate constant ($g\ g^{-1}\ s^{-1}$)
ψ = structure parameter of char (dimensionless)
kC' = rate constant ($g_{NO}\ m^2\ s^{-1}\ atm_{NO}^{-1}$)
n = NO/C ratio in eq 13 or 14 (dimensionless)
M_C = molecular mass of carbon ($g\ mol^{-1}$)

EF800695K